

Ground Water Occurrence and Contributions to Streamflow in an Alpine Catchment, Colorado Front Range

by D.W. Clow¹, L. Schrott², R. Webb³, D.H. Campbell³, A. Torizzo⁴, and M. Dornblaser⁵

Abstract

Ground water occurrence, movement, and its contribution to streamflow were investigated in Loch Vale, an alpine catchment in the Front Range of the Colorado Rocky Mountains. Hydrogeomorphologic mapping, seismic refraction measurements, and porosity and permeability estimates indicate that talus slopes are the primary ground water reservoir, with a maximum storage capacity that is equal to, or greater than, total annual discharge from the basin ($5.4 \pm 0.8 \times 10^6 \text{ m}^3$). Although snowmelt and glacial melt provide the majority of annual water flux to the basin, tracer tests and gauging along a stream transect indicate that ground water flowing from talus can account for $\geq 75\%$ of streamflow during storms and the winter base flow period. The discharge response of talus springs to storms and snowmelt reflects rapid transmittal of water through coarse debris at the talus surface and slower release of water from finer-grained sediments at depth.

Ice stored in permafrost (including rock glaciers) is the second largest ground water reservoir in Loch Vale; it represents a significant, but seldom recognized, ground water reservoir in alpine terrain. Mean annual air temperatures are sufficiently cold to support permafrost above 3460 m; however, air temperatures have increased 1.1° to 1.4°C since the early 1990s, consistent with long-term (1976–2000) increases in air temperature measured at other high-elevation sites in the Front Range, European Alps, and Peruvian Andes. If other climatic factors remain constant, the increase in air temperatures at Loch Vale is sufficient to increase the lower elevational limit of permafrost by 150 to 190 m. Although this could cause a short-term increase in streamflow, it may ultimately result in decreased flow in the future.

Introduction

Alpine areas form the headwaters of most major river systems in the western United States, supplying water for human consumption, agriculture, and industry throughout the region. The seasonal hydrograph in these high-elevation areas is driven primarily by the formation and subsequent melting of deep seasonal snowpacks, and to a lesser extent, summer melt contributions from glaciers and permafrost. Runoff during the snowmelt (May–July) usu-

ally accounts for more than 80% of total annual flow (Kattlemann and Elder 1991; Campbell et al. 1995). Less obvious is the contribution of ground water, which sustains streamflow for the remaining nine months of the year.

The influence of ground water on the hydrology and hydrochemistry of alpine catchments is poorly understood, largely because traditional techniques for studying ground water occurrence and movement are difficult to use. Alpine areas generally lack easy access and commonly are within areas designated or managed as wilderness, precluding use of motorized equipment. Surficial geologic material consists mostly of talus and till, which are coarse-grained and poorly sorted deposits, making manual installation of wells and other subsurface hydrologic equipment impractical.

The coarse-grained nature and steep slopes of most surficial deposits in alpine catchments led to the common assumption that they have little water-storage capacity and that water moves rapidly through the subsurface with little interaction with minerals and biota in soil. These assumptions have not been adequately tested, but have important

¹USGS/WRD, MS 415 Federal Center, Box 25046, Lakewood, CO 80225; 303-236-4882, ext. 294; dwcloy@usgs.gov

²University of Bonn, Germany

³USGS, Denver, Colorado

⁴USGS, Denver, Colorado; now at Ross Environmental Associates Inc., Stone, Vermont

⁵USGS, Boulder, Colorado

Copyright © 2003 by the National Ground Water Association.

implications for the health of high-elevation aquatic ecosystems and for water-resource management. Alpine ecosystems in the Rocky Mountains receive more atmospherically deposited nitrogen than they can assimilate (Williams et al. 1996a; Campbell et al. 2000), and acidic sulfur deposition continues to affect these sensitive ecosystems. Rates of biotic uptake of nitrogen and of acid neutralization by mineral-weathering reactions are dependent on the residence times of water and the physical, chemical, and biological character of surficial geologic deposits.

The hydrology of alpine catchments may be strongly affected by climate change induced by greenhouse gas emissions. Haeberli and Beniston (1998) documented an increase in mean annual air temperature (MAAT) in the European Alps of 1° to 2°C since the early 1980s and noted that glaciers in the region have lost 10% to 20% of their ice volume since 1980. Increases in MAAT are expected to increase the equilibrium line altitude (ELA) of glaciers and the lower limit of permafrost, causing short-term increases in streamflow that will be followed by long-term declines as these surface and subsurface reservoirs of frozen water are depleted. More information about the occurrence and movement of ground water, both liquid and frozen, in alpine areas is needed to gain a better understanding of the potential effects of climate change on alpine hydrology.

In this paper, we present results from a field study of ground water hydrology in Loch Vale, an alpine catchment in the Front Range of the Colorado Rocky Mountains. The objective is to quantify the occurrence and movement of ground water and its contribution to the hydrology of an alpine stream. The distribution and physical characteristics of major hydrogeomorphologic units are described based on mapping, seismic refraction measurements, and soil grain-size analyses. Hydrologic characteristics (hydraulic conductivity, storage capacity) of three ground water spring reservoirs are evaluated based on seasonal variations in flow and water temperature, and on flow-recession analysis of spring discharge data. Spatial and seasonal variations in ground water contributions along a stream reach were quantified using three independent methods, including (1) a tracer-injection experiment, (2) repeated discharge measurements at two sites with no surface inflows between them, and (3) a comparison of continuous discharge measured at gauges on the stream and on a nearby talus-fed spring. Lastly, trends in MAAT at Loch Vale during 1992–2000 are presented, followed by a discussion of possible effects of climate change on alpine hydrology.

Site Description

Loch Vale is a 690 ha catchment located in Rocky Mountain National Park, ~ 100 km northwest of Denver, Colorado (Figure 1). The basin is in an area managed as wilderness and is accessed by a 5 km hiking/skiing trail. The basin is primarily alpine in character, with elevations ranging from 3097 m at the basin outlet to 4009 m at Taylor Peak on the Continental Divide, which forms the western boundary of the basin. Estimated mean annual air temperatures range from 1.7°C at the basin outlet to –5.0°C at Taylor Peak. Mean annual precipitation is 110 cm, with 65% to 85% falling as snow (Baron and Denning 1993).

Two streams, Andrews Creek and Icy Brook, drain alpine valleys in the upper part of the Loch Vale catchment, flowing east from the Continental Divide and merging about 0.5 km above Loch Vale, the lowest of four small lakes in the basin. Stream gauges are operated on Andrews Creek (elevation 3211 m) and Icy Brook (elevation 3164 m) just above where the streams merge, and at the outlet of Loch Vale (Figure 1). Other hydrologic equipment in the basin includes gauges on three ground water springs issuing from the base of talus slopes and three weather stations at elevations ranging from 3150 to 3520 m.

Landscapes in Loch Vale reflect its glacial history. The area that is now Rocky Mountain National Park was heavily glaciated during the Pleistocene, resulting in cirques and steep, U-shaped valleys. Approximately 53% of the basin consists of bare rock exposed on cliffs up to 300 m high and in scattered outcrops on the valley bottoms and sides (Figure 1). Other important landscapes in Loch Vale include talus and debris slopes on the valley sides below the cliffs (17%), blockslopes along the ridge tops (14%), forest in the valley bottoms (7%), rock glaciers (3%) and glaciers (3%) in the cirques, open water (2%), and wetlands and sub-alpine meadows along the valley bottom (1%).

Vegetation in the basin consists of Englemann spruce (*Picea engelmannii*) and supalpine fir (*Abies lasiocarpa*) forest below 3170 to 3350 m and alpine tundra with grasses, sedges, and herbaceous cushion plant communities at higher elevations (Arthur 1992). Talus and debris slopes, blockslopes, and rock glaciers support little vegetation other than lichen. Less than 1% of the Andrews Creek and Icy Brook subcatchments is forested.

Hydrogeomorphologic Setting

Mapping and Seismic Refraction Techniques

The principal ground water storage reservoirs in Loch Vale include talus slopes and debris cones, rock glaciers, blockslopes, glacial till, bedrock, and wetlands. These hydrogeomorphologic units were mapped based on field reconnaissance using digital orthophoto stereo pairs overlaid on a 10 m contour map made from a digital elevation model (DEM) (Table 1). Mapping criteria included geologic and geomorphic features, type and extent of vegetation, and field observations of hydrologic features such as springs and seeps. Hydrogeomorphologic unit boundaries were digitized and converted to a geographic information system (GIS) coverage, allowing calculation of the area covered by each unit.

A 24-channel seismograph was used to estimate the thickness of talus slopes and valley fill deposits in the Andrews Creek and Icy Brook subcatchments (Table 1). Nine seismic refraction profiles were carried out on talus slopes and debris cones, in the valley bottom, and on rock glaciers. For each profile, 10 to 15 shots were made using a 5 kg sledgehammer. Profile lengths ranged from 24 to 69 m, corresponding to a geophone spacing of 2 to 3 m. One-dimensional subsurface models were generated using the intercept-time method (Reynolds 1997). Velocity analysis and calculation of depth of refractors were performed with ReflexW v. 2.5 software (Sandmeier 1998).

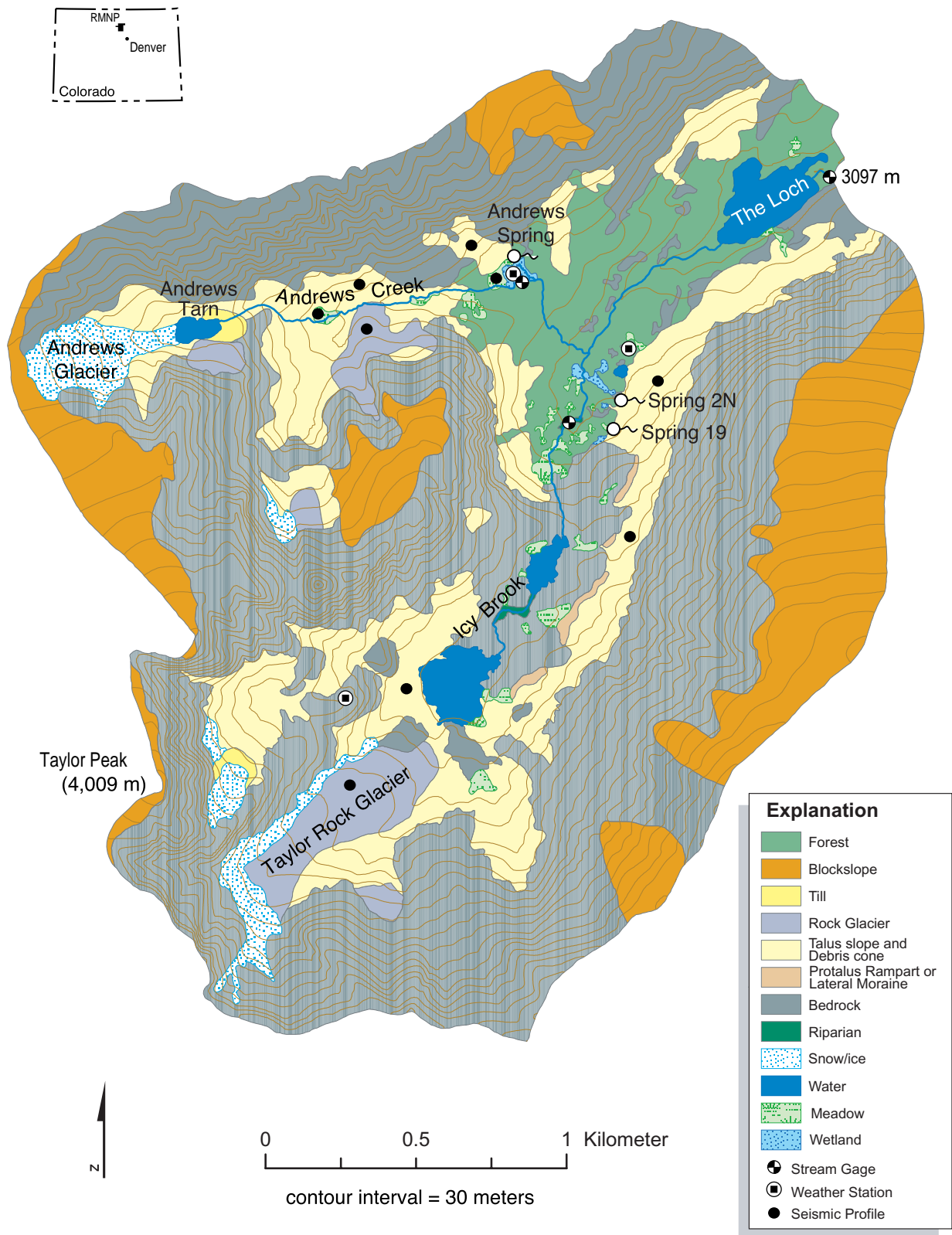


Figure 1. Map showing locations of weather stations, stream gauges, monitored springs, seismic profiles, and distribution of hydrogeologic units in Loch Vale, Rocky Mountain National Park.

Spatial Distribution and Characteristics of Hydrogeomorphological Units

Bedrock

Bedrock in Loch Vale consists of Precambrian biotite schist, which underlies most of the basin, and Precambrian granite, which occurs in three isolated outcrops in the val-

ley bottom and along the northern and southern boundaries (Braddock and Cole 1990). These igneous and metamorphic rocks are resistant and have undergone minimal weathering since their exposure after the last glacial maximum. Matrix porosity of granitic rocks is usually less than 1% with little interconnection between pores, and ground water flow through the bedrock is assumed to take place

Table 1
Summary of Products and Methods Used in This Study

Product	Method(s)
Spatial distribution of units	Hydrogeomorphological mapping
Thickness of surficial material, and of active layer	Seismic refraction
Hydraulic conductivity of surficial material	Grain-size analysis, flow recession analysis
Storage capacity of hydrogeomorphological units	Area × depth × porosity
Area and volume of permafrost	Mean air temperature modeling, GIS analysis
Groundwater storage in Andrews Spring catchment	Flow recession analysis
Groundwater contributions to stream	Tracer experiment, stream and spring gaging
Air temperature trend analysis	Seasonal Kendall Tau

primarily in faults or fractures (Davis 1969). Although there are no major faults in Loch Vale, there are minor northwest-trending vertical faults and fractures in the schist that could provide conduits for ground water flow. The granite is massive, precluding significant fracture flow through it.

Fracture permeability in granitic rocks usually is heterogeneous and decreases quickly with depth (Fetter 2001). Snow (1968) reported data on fracture spacing, aperture, porosity, and permeability measured in boreholes drilled at four dam sites in the Colorado Front Range. Bedrock lithology at the dam sites is similar to that in Loch Vale, consisting of Precambrian granite and granite gneiss. Borehole logs indicated that fracture spacing decreased from 1.5 to 3 m near the surface, to 4.5 to 10.7 m at the 61 m depth; fracture apertures decreased from 80 to 230 μm near the surface, to 40 to 70 μm at 61 m; and fracture porosities decreased from 0.04% near the surface to 0.001% at 61 m (Snow 1968). Hydraulic conductivities, measured using injection tests in the boreholes, decreased logarithmically with depth, ranging from ~10⁻⁴ m/sec near the surface to 10⁻⁷ m/sec at 61 m. Variations in permeability with depth

were substantially greater than variations in permeability among dam sites.

To calculate the storage capacity of bedrock in Loch Vale, we assumed a porosity of 0.04% and open fracture depths of 5 to 10 m (Snow 1968). Results indicate a storage capacity of 6.6 × 10³ to 1.3 × 10⁴ m³ in shallow bedrock in Loch Vale (Table 2), although this probably is an overestimate because bedrock at the dam sites is more extensively weathered than in Loch Vale. Additional water may be stored in deeper fractures, but it probably moves relatively slowly (Kattlemann 1989). Close proximity to the Continental Divide argues against substantial regional ground water flow through the bedrock.

Elongate bedrock outcrops, or roches moutonnées, protrude through the valley till in many places. These low bedrock ridges can dam or divert water moving through the subsurface; the effects are particularly apparent near the base of talus slopes, which discharge ground water to the valley below. A good example is the pond 100 m southeast from the confluence of Andrews Creek and Icy Brook; the pond occurs where discharge from talus cones is blocked by a 5 m high bedrock ridge, forcing water to the surface

Table 2
Estimated Storage Capacities and Hydraulic Conductivities of Bedrock and Surficial Material in Loch Vale

Type of Material	Area (ha)	Range of Estimated Depth (m)	Storage Capacity (m ³ × 10 ³)	Hydraulic Conductivity (m/sec × 10 ⁻³)
Shallow bedrock fractures ¹	330	5 to 10	6.6 to 13	0.01 to 10
Blockslopes ²	46	1 to 3	230 to 690	1.1 to 2600
Glacial till, below timberline ³	33	0.3 to 2.7	20 to 180	4 to 6
Glacial till, above timberline	3	12.3 to 18.6	74 to 110	4 to 6
Talus slopes	132	8.5 to 26.5	5600 to 17,000	6.5 to 9.4
Rock glaciers	30	10 to 20	1500 to 3000	
Non-rock glacier permafrost	77	1 to 3	390 to 1155	
Snow glaciers ⁵	11	10 to 30	2100	
Wetlands ⁴	7	0.3 to 2.7	1.1 to 9.5	0.004 to 0.95

¹Hydraulic conductivity estimated from data in Snow (1968)

²Hydraulic conductivity estimated from data in Davinroy (2000)

³Depth from Baron (1992)

⁴Hydraulic conductivity estimated from data in Bachmann (1994)

⁵Snow glacier area and volume from Baron and Denning (1992)

before moving downvalley through a notch in the bedrock (Figure 1).

Blockslopes

Blockslopes, which form through freeze/thaw weathering of underlying bedrock, occur on ridgetops above the upper limit of late Pleistocene glaciers (Braddock and Cole 1990; Ballantyne 1998). These relatively old deposits consist of angular boulders that are supported in some locations by a matrix of sand and silt, forming diamictons (Ballantyne 1998). Blockslopes generally are less than a few meters thick and have slope angles that typically range from 1° to 35° in the Front Range (Ballantyne 1998; Davinroy 2000), and 15° to 35° in Loch Vale. Blockslopes in Loch Vale tend to develop only minimal snow cover during winter due to high wind speeds on the ridges, and substantial ground water recharge and flow occurs in them only during summer rainstorms.

Porosities of blockslopes in Loch Vale have not been measured, but are likely to be near 50% based on measurements on similar deposits in the Colorado Front Range (Davinroy 2000) and in New Zealand (Pierson 1982). The steep slopes and high porosities of blockslopes result in high hydraulic conductivities. Dye tracers were used to measure flow velocities of 1.8 to 2.6 cm/sec through coarse debris on blockslopes in the alpine portion of Green Lakes Valley, 30 km south of Loch Vale (Davinroy 2000). Constant head permeameter tests in blockslopes containing fine material (<2 mm) indicated hydraulic conductivities ranging from 1.1×10^{-3} to 3.9×10^{-3} m/sec (Davinroy 2000). Infiltration tests indicated permeability was sufficient to preclude development of overland flow during any likely precipitation event. The estimated storage capacity of blockslopes in Loch Vale is 2.3×10^5 to 6.9×10^5 m³ (Table 2), based on an assumed porosity of 50% and depths ranging from 1 to 3 m (Table 2). The largest uncertainty in the calculation of storage capacity of blockslopes and other surficial materials in Loch Vale is sediment depth, which is spatially variable and difficult to measure. Using a range of depths provides reasonable boundaries for the estimates.

Late Pleistocene Till

Receding late Pleistocene glaciers left patchy till deposits in the valley bottoms of Loch Vale. These deposits are composed of subangular to subrounded boulders and cobbles supported by a silty sand or sandy silt matrix (Gable and Madole 1976). Seismic refraction measurements in the till below timberline indicated a depth of 1.5 ± 1.2 m to bedrock (mean ± 1 standard deviation, $n = 37$) (Baron 1992). Our seismic refraction measurements in the till above timberline indicate it is much deeper, with depths ranging from 12.3 to 18.6 m (Table 2). Typical p-wave velocities in the till above timberline vary from 850 to 1400 m/sec. In the till above timberline, an increase in p-wave velocity at a depth of several meters indicated a transition from uncompacted to compacted sediments.

Hydraulic conductivities for Loch Vale till were estimated based on grain-size distributions, using the method of Masch and Denny (1966) (Table 1). Estimated hydraulic conductivities of till ranged from 4×10^{-3} to 6×10^{-3} m/sec (Table 2). Although these hydraulic conductivities

are higher than for most tills, they are reasonable for tills derived from mountain glaciers, which tend to deposit very coarse material (Fetter 2001). Storage capacities of till above and below timberline were estimated separately due to the large differences in average depth, using an assumption of 20% porosity (Fetter 2001). Estimated storage capacities of till above and below timberline were similar to each other and were on the order of 10^4 to 10^5 m³ (Table 2).

Talus Slopes and Debris Cones

The most extensive surficial deposits in Loch Vale are talus slopes, which can be subdivided into talus cones and talus sheets. More than 95% of talus slope deposits in Loch Vale are talus cones, which form steeply sloping (33° to 40°), fan-shaped deposits at the base of cliffs. Talus cones accumulate through rockfall and granular disintegration of cliff faces, which is promoted by freeze/thaw processes acting in fractures and along grain boundaries (Lautridou 1988). Rockfall is funneled down steep gullies called couloirs, impacting talus cones near the apex and often rolling to the bottom, creating a highly permeable open-work structure at the base. Sand and gravel also tend to be funneled down through couloirs and deposited near the apex of the cone. This finer material may be transported downslope by sheetwash or debris flows (Schrott et al. 2003), but in general it tends not to travel as far as larger blocks, so grain size tends to increase downslope (Lautridou 1988). Talus sheets are similar to talus cones in grain size, internal structure, and location (below cliffs), but form broad sheets rather than cones.

Cross sections through talus cones in Loch Vale, Green Lakes Valley (Davinroy 2000), and Scotland (Lautridou 1988) indicate several modes of internal structure. Open-work structures composed of large clasts are common at the base of talus cones and as surface layers overlying diamictons. The diamictons may be clast-supported or matrix-supported, depending on the degree of infilling by fine debris. Hydraulic conductivities decrease and storage capacities increase as the proportion of fine material in the deposits increases. Hydraulic conductivities estimated for the fine fraction of talus soils in Loch Vale range from 6.5×10^{-3} to 9.4×10^{-3} m/sec on the basis of grain-size distributions. These values represent minimum estimates for talus soils because they do not take into account macropores or open-work structures that are known to exist.

The depth of talus-cone sediments was measured at four locations using seismic refraction (Figure 1). Three sets of measurements were made near the middle of the cones to determine maximum sediment thickness, and one set of measurements was made in the interfluvium between cones to determine minimum sediment thickness. Results indicate talus-cone sediment thickness ranged from 8.5 to 26.5 m (Table 2). P-wave velocities of talus-cone sediments range from 400 to 1600 m/sec. The lower values, which occurred in the upper few meters, are typical of unconsolidated layers containing sand and coarse debris. An increase in velocities to between 1100 and 1600 m/sec indicated a more dense compaction of the talus cones with depth. The transition to bedrock was indicated by velocities

between 3600 and 6170 m/sec, which are typical of values for metamorphic rocks.

Talus porosity was estimated on the basis of measurements made on similar deposits in Green Lakes Valley and in New Zealand. Porosity of talus in Green Lakes Valley ranged from 43% to 60% (Davinroy 2000), which is similar to values reported for scree slopes in New Zealand (Pierson 1982). If we assume 50% porosity and sediment thickness of 8.5 to 26.5 m for Loch Vale talus, we obtain a storage capacity estimate of 5.6×10^6 to 1.7×10^7 m³ (Table 2). These values are an order of magnitude larger than for any of the other hydrogeomorphologic units in Loch Vale (Table 2) and are equal to, or greater than, the average annual discharge at the Loch Vale outlet ($5.4 \pm 0.8 \times 10^6$ m³ for 1984–2000; data available at www.nrel.colostate.edu/projects/lvws/). It should be recognized, however, that it is unlikely that the entire storage capacity of talus slopes is ever filled because of their high porosities and hydraulic gradients.

Debris cones are similar in hydrogeomorphic character to talus slopes and thus were mapped as a single unit. They accumulate through debris flow, rockfall, and sheetwash processes (Schrott et al. 2003). Their areal coverage is much smaller than that of talus cones in Loch Vale.

Rock Glaciers and Permafrost

Rock glaciers are a form of mountain permafrost (Barsch 1978; Harris and Corte 1992) and may constitute an important, but seldom recognized, ground water reservoir in alpine terrain (Schrott 1996). At least four active rock glaciers occur in high-elevation cirques in Loch Vale; the modes of formation of these deposits are complex and controversial, but their general character involves mixtures of rock and ice. Coring through rock glaciers in the Swiss Alps indicates that the internal structure is characterized by an outer mantle of coarse debris (the active layer) and an inner core of frozen sand and gravel with ice content of 50% to 80% (Barsch 1988). Water formed from the melting of ice-rich permafrost forms supraglacial channels at the contact between the active layer and the frozen permafrost body, which is essentially impermeable.

The largest rock glacier in Loch Vale is Taylor Rock Glacier, which is ~250 m wide, 750 m long, and at least 30 m thick in places (Figure 1). Seismic refraction data on Taylor Rock Glacier, and on another large rock glacier in the Andrews Creek drainage, indicated the thickness of the active layer ranges from 2.6 to 4.5 m. Assuming an average permafrost thickness of 10 to 20 m with an ice content of 50%, the volume of ice stored in rock glaciers is 1.5×10^6 to 3.0×10^6 m³. This volume is similar to that estimated for snow glaciers in Loch Vale (2.1×10^6 m³; Table 2) by Baron and Denning (1992).

Rock glaciers are not the only form of permafrost in Loch Vale. Permafrost can occur in talus and blockslope material that is subfreezing much of the year; ice stored in this type of permafrost may represent an additional ground water storage reservoir. MAATs of -1°C have been shown to approximate the lower limit of discontinuous permafrost in the Front Range and in the Swiss Alps (Barsch 1978). To determine the potential distribution of permafrost in Loch

Vale, MAATs for the 1992–2000 water years (October–September) were modeled on a 30 m grid using the Image Processing Workbench (Frew 1990) and the algorithms outlined in Funk and Hoelzle (1992) and Swift (1976). These algorithms estimate MAATs based on variations in solar radiation attributable to latitude and to differences in slope, aspect, and shading, which are derived from a digital elevation model. MAATs were adjusted for variations in air temperature with elevation, using lapse rates measured at the Loch Vale weather stations.

The -1°C isotherm in Loch Vale occurs at an elevation of ~3460 m, but its position varies as a function of slope, aspect, and distance from cliff walls, which reduce incoming radiation through shading. On north-facing slopes, which are relatively cold, the -1°C isotherm occurs at 3310 m. On south-facing slopes, the -1°C isotherm occurs at 3612 m. These results are consistent with permafrost lower limits indicated by minimum rock glacier elevations in Loch Vale, which occur at elevations ranging from 3360 to 3440 m. At Niwot Ridge, Ives (1973) reported that permafrost was extensive at elevations above 3750 m.

Snow cover is a critical variable in determining the distribution and thickness of permafrost due to its insulating properties (Keller and Gubler 1993). In Loch Vale, as well as elsewhere in the Colorado Front Range, permafrost is unlikely to form where deep seasonal snowpacks insulate the ground during most of the winter. Digital orthophotos of snow-covered areas, which were available for 1994, were overlaid on the MAAT map to identify places in Loch Vale where permafrost is likely (Figure 2). Those areas

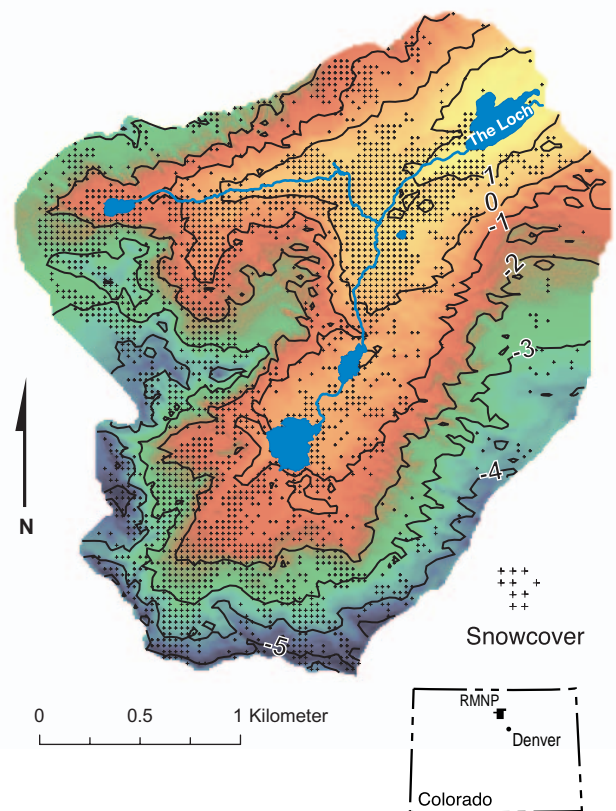


Figure 2. Simulated mean annual air temperatures in Loch Vale.

predominantly are wind-scoured locations above timberline on northeast- through northwest-facing slopes.

The area of non-rock glacier (NRG) permafrost was calculated by taking the area of the Loch Vale basin having MAATs $\leq -1^{\circ}\text{C}$ (462 ha) and subtracting the fraction of that area with significant winter snow cover (rock glacier area was excluded because ice volume estimates are provided separately). Of the remaining 239 ha, 162 ha is underlain by bedrock, which cannot store significant amounts of water. Thus, NRG permafrost is likely to occur in 77 ha, or 11% of the Loch Vale basin. Assuming an average depth of 1 to 3 m and a porosity of 50% for the surficial geologic deposits underlying areas with NRG permafrost, the storage capacity of those deposits is 0.39×10^6 to $1.1 \times 10^6 \text{ m}^3$ (Table 2). This estimate indicates only the maximum amount of ice that could be stored in NRG permafrost; only a fraction of that storage capacity is likely to be filled with ice because of the high porosities of block-slopes and talus cones.

Wetlands

Wetlands occur in Loch Vale in areas of ground water discharge, mostly along the valley edge at the base of talus slopes. The wetlands formed through the accumulation of peat on shallow slopes where organic-rich soils could become established after deglaciation. A study of wetland hydrology in Loch Vale by Bachmann (1994) documented that surface flows accounted for 90% to 99% of flow through wetland areas, and flow through the subsurface was minimal. Most flow through the wetland landscape originates as discharge from springs at the base of talus slopes above the wetlands. Hydraulic conductivities of the wetland peat are low compared to other surficial materials in Loch Vale, ranging from 4.4×10^{-6} to $9.5 \times 10^{-4} \text{ m/sec}$ based on constant-head permeameter tests (Table 2) (Bachmann 1994). Ground water gradients measured using an array of wells tended to follow the underlying bedrock topography (Bachmann 1994). This probably is true for other hydrogeomorphic units in Loch Vale as well. We estimate the storage capacity of wetlands to be 1.1×10^3 to $9.5 \times 10^3 \text{ m}^3$, assuming 20% porosity and depths between 0.3 and 2.7 m (Table 2).

Hydrologic Behavior of Ground Water Springs

Field observations of spring water flow emanating from the base of talus cones in Loch Vale suggest that these "talus springs" may be an important source of water and solutes to alpine surface waters, particularly during fall through early spring, when snowmelt contributions are minor. To quantify talus spring discharge, stage and water temperature were monitored continuously at two springs (Andrews Spring and Spring 19) from October 1996 through September 2002, and at a third spring (Spring 2N) from October 1997 through December 1998 (Figure 1). Discharge was calculated using a stage-discharge equation applicable to 90° v-notch weirs (Rantz 1982), which were installed at each of the three spring-monitoring sites. Andrews Spring and Spring 19 flow from rubble at the base of south- and northwest-facing slopes, respectively. Spring

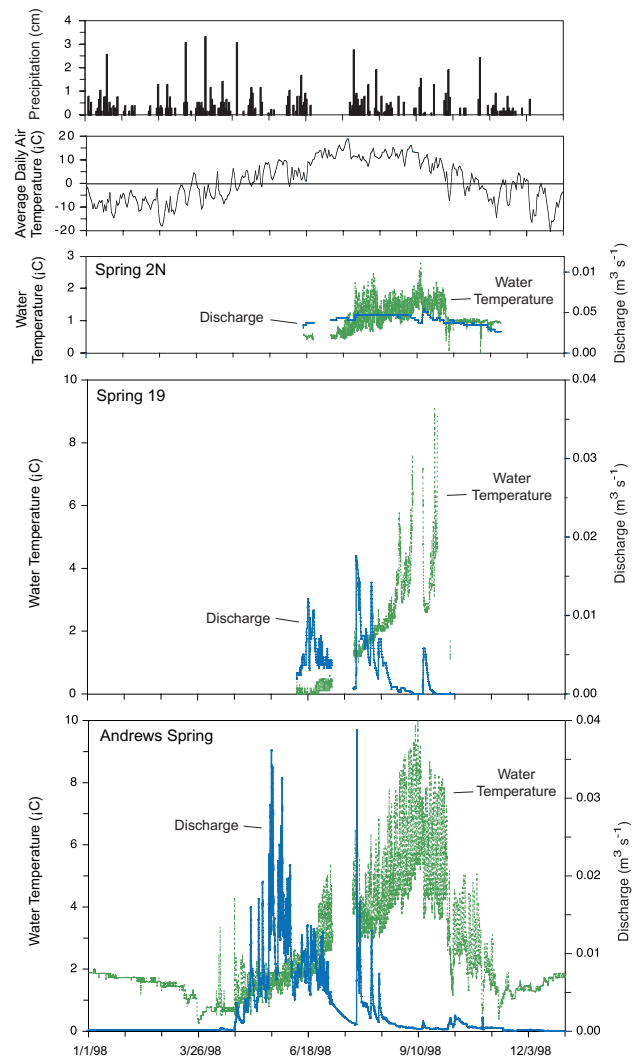


Figure 3. Daily precipitation and daily average air temperatures at 3215 m elevation, and 15-minute average discharge and spring water temperatures at Spring 2N, Spring 19, and Andrews Spring in 1998.

2N flows from a subhorizontal fracture in a bedrock outcrop below a northwest-facing slope.

There were substantial differences in the magnitude and duration of flow at the three ground water springs (Figures 1 and 3). Andrews Spring had the highest discharge of the three springs, and it flowed throughout the year. The other two springs did not flow during winter. In most years, Spring 19 began flowing during the first week in May and flowed until late summer, when a seasonal snowfield disappeared and a soil moisture deficit developed. Some late summer rainstorms, such as the storm in early September 1998 (Figure 3), provided enough moisture to overcome the moisture deficit and temporarily reinstate flow at Spring 19. Spring 2N generally flowed from early June through October, and showed much smaller responses to snowmelt and storms than the other two springs.

Continuous water temperature data provide information about possible sources and flowpaths of spring water. Water temperatures at Andrews Spring and Spring 19 showed strong diurnal variations and a gradual increase through the summer (Figure 3). These data indicate the spring water follows a shallow flowpath, where daily and

seasonal variations in solar heating are felt. Andrews Spring and Spring 19 water temperatures varied inversely with discharge, probably reflecting a decrease in flow velocity and an increase in residence time in warm, shallow soil during summer low flow. At Spring 2N, the overall seasonal variation in water temperature was much smaller and water temperatures were much colder than at the other springs. The cold temperatures and relative invariance of discharge and temperature suggest that melting of buried ice (possibly permafrost) may be the main source of water at Spring 2N. Although a deep flowpath also could explain the invariance of discharge and water temperature, it is not consistent with cessation of flow during winter.

Ground water storage in the Andrews Spring basin was calculated using the base-flow recession method outlined in Fetter (2001) and Vitvar et al. (2002) (Table 1). After a storm, if new contributions from snowmelt and rain are minimal, discharge decays exponentially as ground water drains from the subsurface reservoir (Figure 3). The shape of the base-flow recession hydrograph depends on topography and the physical characteristics of subsurface materials, and may be modeled using the following equation:

$$Q_t = Q_0 e^{-\alpha t}$$

where Q_0 is flow at time $t = 0$, Q_t is flow at a later time t , and α is a recession coefficient for the basin (Fetter 2001). Ground water storage (S_g) is the amount of water released from the ground water reservoir after the storm peak, and is calculated as

$$S_g = Q_0 t / \alpha$$

A spatially integrated hydraulic conductivity (K) may be calculated by rearranging the Darcy's law equation:

$$K = -Q / \{A (dh/dL)\}$$

where Q is discharge, A is the cross-sectional area of the aquifer, and dh/dL is the hydraulic gradient. A is calculated as

$$A = S_g (\text{aquifer width}) / \{(\text{porosity})(\text{aquifer area})\}$$

The size of the aquifer area is constrained by surrounding bedrock outcrops and was calculated from the hydrogeology coverage using standard GIS tools. Lacking wells in the talus, we estimated the hydraulic gradient from surface and bedrock topography using the DEM and seismic refraction data. The Andrews talus cone rises 61 m over a distance of 250 m, so the upper limit for the hydraulic gradient is 0.24. If we assume an average depth to bedrock of 20 m, then the lower limit for the hydraulic gradient is 0.16.

Base-flow recession analysis was performed on six base-flow periods during the 1997–2002 water years. Ground water storage ranged from 22,939 to 166,381 m³, reflecting differences in rainfall inputs, antecedent moisture conditions, and the duration of the base-flow recession period (Table 3). The larger value may be close to the maximum storage capacity of the talus cone because it is based on a long recession period (196 days) after a particularly wet summer. The thickness of aquifer material drained during the base-flow recession periods ranged from 1.5 to 11.2 m (Table 3). These values appear reasonable when compared to the total thickness of the talus deposits calculated from the seismic refraction measurements on the Andrews talus cone (18 to 22.5 m).

Hydraulic conductivity estimates ranged from 8.0×10^{-6} to 4.4×10^{-4} m/sec and α estimates ranged from 0.77 to 0.98 (Table 3). Variations in the estimates for K and α probably reflect variations in grain size and porosity with depth (both decrease with depth); a temporally varying water table depth results in temporally varying aquifer

Table 3
Aquifer Parameters for Andrews Spring Basin Derived From Flow Recession Analysis

Date	Discharge m ³ /sec	α	Storage m ³	K_1 m/sec	K_2 m/sec	Aquifer Thickness Drained (m)
8/10/97	0.0428	0.77	73,856	3.0×10^{-4}	4.4×10^{-4}	5.0
8/25/97	0.0007			1.0×10^{-4}	1.5×10^{-4}	
9/23/97	0.0096	0.98	166,381	3.0×10^{-5}	4.4×10^{-5}	11.2
4/8/98	0.0001			8.0×10^{-6}	1.2×10^{-5}	
8/10/98	0.0074	0.91	22,939	1.7×10^{-4}	2.5×10^{-4}	1.5
9/12/98	0.0003			1.4×10^{-4}	2.0×10^{-4}	
8/6/99	0.0100	0.93	41,689	1.2×10^{-4}	1.8×10^{-4}	2.9
9/19/99	0.0003			7.9×10^{-4}	1.2×10^{-4}	
8/29/00	0.0142	0.83	30,248	2.4×10^{-4}	3.6×10^{-4}	2.1
9/19/00	0.0003			1.1×10^{-4}	1.6×10^{-4}	
5/30/02	0.0113	0.92	42,007	1.4×10^{-4}	2.0×10^{-4}	2.9
7/9/02	0.0004			9.9×10^{-5}	1.5×10^{-4}	

α is a recession coefficient for the basin. Hydraulic conductivities, K_1 and K_2 , were calculated using estimated hydraulic gradients of 0.24 and 0.16, respectively.

parameters (K and α). The long base-flow recession during winter 1997–1998 provided the lowest K and highest α estimates. The August 1997 storm provided the highest K and lowest α estimates. We hypothesize that the water table depth is relatively low during winter. The low K estimate for winter reflects drainage from relatively compact, low-porosity talus sediments at depth; the high α estimate reflects the flatness of the recession curve. During summer storms, the water table rises into shallower, less compact sediments with higher porosity and larger grain size; water transmittal through the shallow talus sediment is rapid and the water table depth changes rapidly in response to storms, as reflected in the high K and low α estimates for summer storms.

Quantifying Ground Water Contributions

Tracer Experiment Methods

A continuous-injection tracer experiment was conducted during September 1998 on an 838 m reach of Andrews Creek under base-flow conditions to quantify lateral inflows and interactions between the main stream channel and transient storage zones (Table 1). Quantification of lateral inflows (surface and subsurface) allowed us to determine the locations of ground water inflows to Andrews Creek. Quantifying exchange between the main channel and transient storage areas, such as eddies, pools, and the coarse gravel and cobble in the streambed, is important for understanding the hydrology of mountain streams (Bencala and Walters 1983). The hyporheic zone is a particularly important component of transient storage because it represents the interface between surface water and ground water, where strong contrasts in solute and gas concentrations promote rapid chemical and biological reactions (Boulton et al. 1998; Battin 1999).

Andrews Creek originates at the outlet to Andrews Tarn, a small pond at the base of Andrews Glacier. The tracer-injection site was at an elevation of 3328 m, about 250 m downstream from the tarn outlet. The creek follows a steep, rocky channel underlain by glacial till, dropping 117 m over a distance of 838 m (slope = 0.14). It flows beneath a rock glacier from 150 to 300 m below the injection point.

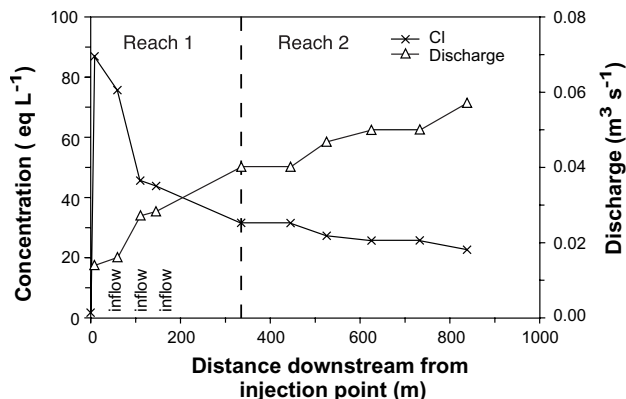


Figure 4. Changes in chloride (Cl) concentrations and discharge with distance from the injection point during tracer experiment.

tion point. The streambed is mostly compacted cobbles and gravel, except for a few pools, which have sandy bottoms. Surface inflows include two spring-fed tributaries flowing from the north that join the main stem at 63 and 111 m downstream from the injection site and a third tributary flowing from the south through large, rock glacier-derived rubble that joins the main stem approximately 161 m downstream from the injection site (Figure 4).

A synoptic survey of the main stem and surface inflows was conducted the day before the tracer experiment to establish background concentrations of the tracer. The tributary flowing from the south could not be sampled because it flows through large rubble at the base of the rock glacier. Ten sites along the main stem were sampled, each defining the lower end of a stream segment.

The tracer experiment began at 8:50 A.M. on September 16, 1998, under base-flow conditions; diurnal variations in flow were minimal. A 47.7 gL^{-1} potassium chloride (KCl) solution was injected for seven hours at a rate of $53.3 \pm 3.4 \text{ mL/min}$. Stream water samples were collected at the lower end of each stream segment after chloride concentrations had reached a steady state. Discharge was calculated for the lower end of each stream segment, based on dilution of chloride in the injected-tracer solution using the following equation:

$$Q = (Q_i C_i) / (C_p - C_b)$$

where Q is stream discharge (L/sec), Q_i is the injection rate (L/sec), C_i is the injectate concentration ($\mu\text{eq/L}$), C_b is the background concentration of tracer ($\mu\text{eq/L}$), and C_p is the steady-state concentration of tracer ($\mu\text{eq/L}$). After accounting for surface inflows, ground water inflows were calculated as the change in discharge between stream segments.

Two reaches selected for more intensive study were sampled every 15 minutes using automatic samplers. The reaches extended from 0 to 335 m (Reach 1) and 335 to 838 m (Reach 2) below the injection point. The lower end of Reach 2 coincides with the Andrews Creek stream gauge. The One-dimensional Transport with Inflow and Storage model (OTIS-P) was used to characterize advection and dispersion in the main channel and exchange between the main channel and transient storage zones (Runkel 1998). Model parameters for dispersion (D), stream cross-sectional area (A), transient storage cross-sectional area (A_s), and the transient storage exchange coefficient (α) were determined using the nonlinear, least squares regression algorithms in OTIS-P (Runkel 1998).

Tracer Experiment Results

Stream discharge increased from $0.014 \text{ m}^3/\text{sec}$ at the top of Reach 1 to $0.041 \text{ m}^3/\text{sec}$ at the bottom of Reach 1, and $0.057 \text{ m}^3/\text{sec}$ at the bottom of Reach 2 (Figure 4). Sub-surface inflows could not be separated from surface inflows along Reach 1 because the short distances between surface inflows precluded adequate mixing of the tracer until near the bottom of each stream segment. Along Reach 2, which had no surface inflows, subsurface inflows contributed ground water to the stream and accounted for $0.016 \text{ m}^3/\text{sec}$, or 30% of total flow in the stream at the lower end of the reach (Figure 4).

Subsurface inflows along Reach 2 probably are derived from drainage from talus cones on both sides of the creek. These deposits have substantial storage capacity and are in close proximity to the creek. The sources of water for the two springs contributing to Reach 1 probably are different. The flow of water coming from the springs is anomalously large, considering the small drainage area directly above the springs. The chemistry of spring water entering the creek at 63 and 111 m below the injection point is similar to that of the creek above the springs and to that of the tarn outlet. The chemical similarity and the large volume of water emanating from the springs suggest that their origin could be Andrews Tarn, and the springs may represent “pipe flow” from the tarn. Subsurface drainage of the tarn is supported by field observations documenting a drop in the water level of the tarn of more than 1 m below its surface outlet during late fall, which is far greater than can be explained by evaporation. A large fraction of discharge in Andrews Creek probably is meltwater from snow on and ice in Andrews Glacier. Discharge in Andrews Creek just below its confluence with the springs provides an upper bound to glacial meltwater inputs. Discharge at that site, which was 145 m below the tracer-injection site, was 0.027 m³/sec or 54% of total flow at the Andrews Creek gauge.

Intensive sampling at the lower ends of Reach 1 and Reach 2 indicated that it took 50 minutes for the tracer to travel the first 335 m and another 65 minutes for the tracer to travel the remaining 503 m to the lower end of Reach 2 (Figure 5). These travel times correspond to stream velocities of 0.11 m/sec in the upper reach and 0.13 m/sec in the lower reach. The decrease in the steady-state chloride concentration measured at 838 m compared to that at 335 m is due to dilution by ground water inflows and to dispersion of the tracer in the stream. A slight rounding of the shoulders of the concentration plateau (Figure 5) indicates dispersion or exchange between the main channel and transient storage areas, such as eddies, pools, and the coarse gravel and cobbles in the streambed (Bencala and Walters 1983). Transient storage also has the effect of increasing the mean residence time of solutes in the stream, as solutes temporarily leave the main channel and reenter it a short time later (Broshears et al. 1993).

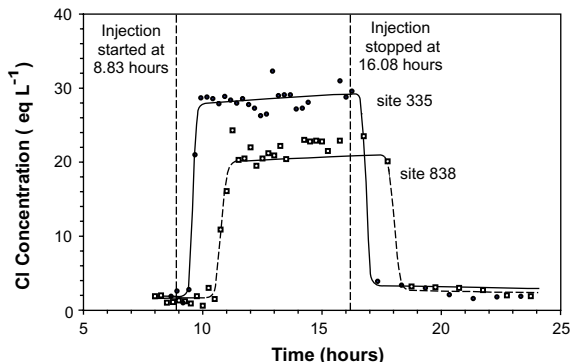


Figure 5. Changes in chloride (Cl) concentrations over time at site 335 and site 838 (the Andrews Creek gauge) during tracer experiment. Simulated Cl concentrations are indicated by solid and dashed lines.

	D (m ² /sec)	A (m ²)	A _s (m ²)	α (s ⁻¹)
Reach 1	0.40	0.22	0.66	5.5 × 10 ⁻⁵
Reach 2	0.05	0.29	0.12	3.8 × 10 ⁻³

Various metrics have been used to evaluate the effect of transient storage on solute transport; one common metric is the ratio of transient storage cross-sectional area to stream cross-sectional area (A_s/A). A large A_s/A indicates a relatively large transient storage zone. Fluxes between the main channel and transient storage also are influenced by the rate of exchange between the main channel and transient storage zones, as described by the transient storage exchange coefficient (α). Simulation results for Andrews Creek indicate that A_s/A was relatively large in the upper reach and much smaller in the lower reach (Table 4). In contrast, α was small in the upper reach and much larger in the lower reach (Table 4). These results indicate that in Reach 1 there was a relatively large, but slow-mixing, transient storage zone, perhaps in the glacial till beneath the streambed. In Reach 2, the results indicate a relatively small, rapidly mixing transient storage zone. Transient storage in Reach 2 may occur as rapid flow through pools or the cobble substrate on the streambed. The parameter values obtained for the Andrews Creek simulations are within the ranges reported for other small, high-gradient streams during base-flow conditions except for α in Reach 2, which is at the high end of the range (Bencala and Walters 1983; Broshears et al. 1993).

Seasonal Variations in Ground Water Contributions

Seasonal contributions of ground water to Andrews Creek were quantified by measuring discharge at the upper boundary (site 335) and the lower boundary (site 838) of Reach 2 during the snow-free period of 1999, using current meter techniques (Rantz 1982) (Table 1). Discharge ranged from 0.011 to 0.129 m³/sec at site 335 and from 0.029 to

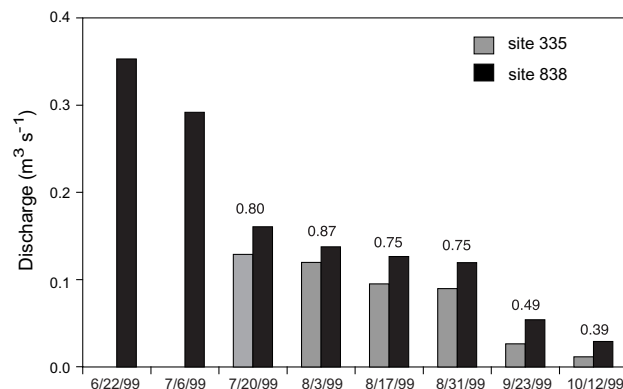


Figure 6. Variations in discharge at site 335 and site 838 during summer 1999. Discharge was not measured at site 335 on June 22, 1999, or July 6, 1999, because of snow cover. Values above columns indicate the ratio of discharge at site 335 to that at site 838.

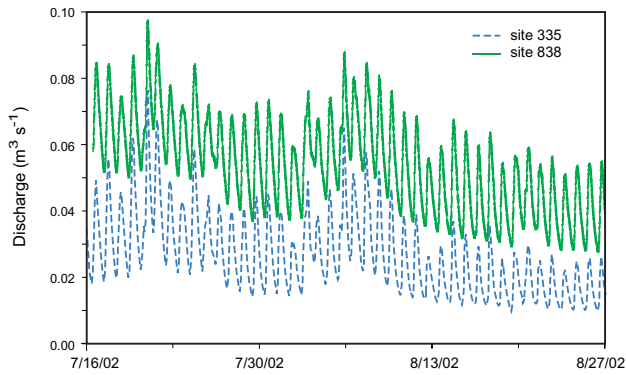


Figure 7. Discharge in Andrews Creek at site 335 and site 838 during summer 2002.

0.161 m³/sec at site 838 (Figure 6), and discharge was less at the upper site than at the lower site in each instance. Differences in discharge between sites ranged from 0.018 to 0.032 m³/sec. This provides an indication of the magnitude of ground water inflows to Andrews Creek along Reach 2. These values are close to the 0.02 m³/sec previously estimated for base flow at site 838 using hydrograph separation techniques (Mast et al. 1995). The ratio of discharge at site 335 to that at site 838 in 1999 ranged from 0.39 to 0.87, and the ratio declined through the summer (Figure 6). This seasonal pattern probably is due to declining snowmelt inputs as seasonal snowfields shrank, as well as to declining melt-water inputs from glaciers and permafrost as temperatures cooled in the fall.

Continuous discharge data collected at site 335 and at site 838 during summer 2002 indicated a strong diurnal signal, with peak flows between 5 and 7 P.M. and minimum flows between 9 and 11 A.M. (Figure 7). Minimum and maximum flows occurred 15 to 45 minutes earlier at site 335 than at site 838, indicating a mean stream-water velocity of 0.2 to 0.5 m/sec. The diurnal signal probably is due to variations in melt rates of ice in the glacier and firn fields; highest melt rates are expected in the afternoon when solar radiation is at its maximum.

The continuous discharge data from summer 2002 indicate the ratio of discharge at site 335 to that at site 838 usually was between 0.35 and 0.60, similar to the values obtained from the instantaneous discharge measurements during 1999 (Figure 7). Rainstorms on July 20 and August 5, 2002, caused the discharge ratio to increase to 0.90 and 0.75, respectively (Figure 7). The increase in the discharge ratio indicates a relatively rapid hydrologic response in the upper part of the Andrews Creek basin. The rapid response may reflect the very large average grain size and high permeability of material in the upper Andrews Creek basin, where car-size boulders are prevalent at the surface.

A comparison of discharge at Andrews Spring to that at Andrews Creek provides additional information about seasonal patterns in talus ground water contributions to stream-flow. Discharge at Andrews Spring is a small fraction of that in Andrews Creek for most of the year (Figure 8). The ratio of Andrews Spring discharge to Andrews Creek discharge increases substantially during late winter, however, approaching 1 in late April to early May. The ratio also increases substantially during storms. These patterns indi-

cate that ground water discharge from talus is the dominant source of water in the creek during winter and during storms.

Possible Effects of Climate Change

Permafrost and other periglacial landforms are highly sensitive to climate change (Haeberli et al. 1993). Air temperature is a driving variable influencing the lower limit of permafrost (Hoelzle and Haeberli 1995), although other climatic factors such as amount and distribution of winter snowfall can be important (Hoelzle and Haeberli 1995; Haeberli and Beniston 1998). Trend analyses were performed on mean monthly air temperatures for 1992–2000 at the three Loch Vale weather stations using the Seasonal Kendall Tau (SKT) test, a nonparametric, seasonally adjusted trend test (Hirsch et al. 1982) (Table 1). Mean monthly air temperatures increased by 0.12° to 0.15°C/year during the period (Table 5), and temperature increases were greatest during summer, when they would have the greatest effect on permafrost melting (Figure 9). These results are consistent with modeling of air temperatures under a doubled CO₂ scenario using the RegCM2 regional climate model, which indicated that increases in air temperature will be most pronounced during summer (Haeberli and Beniston 1998).

Increasing air temperatures during the 1990s at Loch Vale are consistent with longer-term records from many other high-elevation sites in the European Alps, the Peruvian Andes, and the Colorado Front Range. Air temperatures in the European Alps have increased by 0.05° to 0.1°C/year since the early 1980s (Haeberli and Beniston 1998). In the Peruvian Andes, air temperatures have increased by 0.32° to 0.34°C/year since the mid-1970s (Vuille and Bradley 2000). At Niwot Ridge, mean air temperatures at a forested site (3048 m elevation) correlated strongly with those at Loch Vale (*r*-square ≥ 0.71; 1992–2000), and mean annual air temperatures increased 0.07°C/year during 1976–2000 (*p* < 0.001 using SKT). However, at the Niwot Ridge alpine site (3750 m elevation), although long-term patterns in air temperature were similar to those at the forested site (slight decrease during 1953–1975 and a slight increase since then), there were no statistically significant trends. This suggests that air temperature trends can be complex and locally variable. The trends at most of these high-elevation sites are consistent with positive global land surface air temperature trends since 1976 (0.015°C/year [IPCC 2001]), although the magnitude of trends at mountain sites have generally been greater.

Table 5
Results of Seasonal Kendalls Tau Trend Tests on Loch Vale Air Temperature Data, 1992–2000

Parameter	Weather Station Elevation		
	3150 m	3215 m	3520 m
slope (°C/yr)	0.12	0.14	0.15
p-value	.059	.002	.007

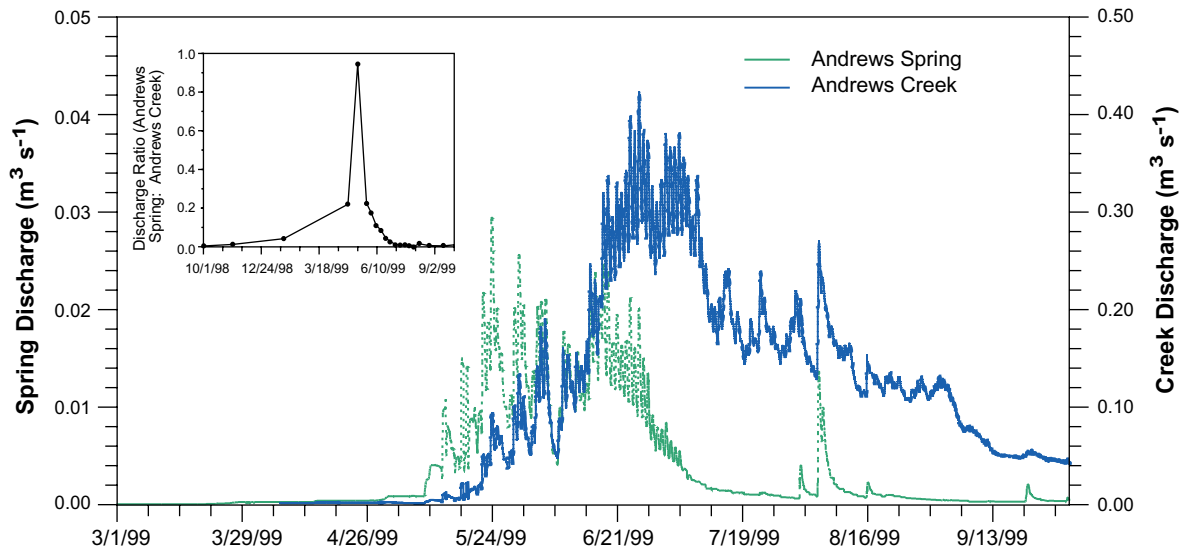


Figure 8. Discharge at Andrews Spring and at Andrews Creek in 1999.

Haeberli and Beniston (1998) and Hoelzle and Haeberli (1995) note that rising air temperatures are likely to increase the lower elevational limits of permafrost in the Alps by several hundred meters, causing changes in the hydrologic cycle and in the distribution and makeup of the vegetative community. Increases in the lower limit of permafrost and decreases in its areal extent have been documented in China (Wang et al. 2000). In Loch Vale, the increase in air temperatures of 1.1° to 1.4°C measured over a nine-year period is sufficient to increase the lower limit of permafrost by approximately 150 to 190 m, suggesting that the hydrology of the basin could be strongly affected by climate change. Changes in the equilibrium line altitude of glaciers also are possible, although climate controls on

glacier mass balance are relatively complex. Increases in snowfall, which have been noted at the alpine site on Niwot Ridge (Williams et al. 1996b), could offset the effect of increasing temperatures (Dyrgerov and Meier 2000).

Conclusions

Talus slopes are the primary ground water reservoir in Loch Vale, having a maximum storage capacity approximately equal to that of total annual discharge from the basin ($5.4 \pm 0.8 \times 10^6 \text{ m}^3$). Hydraulic conductivities in talus and in the other hydrogeomorphological units are highly variable, reflecting differences in grain size and in the structure and compaction of the sediments. Coarse, open-work structures provide conduits for rapid flow, and underlying finer-grained sediments release water more slowly, providing water that maintains base flow in streams through fall and winter. Results from a tracer test and from discharge measurements on an alpine stream and a nearby talus spring indicate that drainage of water from talus fields can account for more than 75% of streamflow during storms and during the fall and winter base-flow period.

Ice stored in permafrost (mostly in rock glaciers) is approximately equal in volume to that stored in snow glaciers in Loch Vale. The ice in rock glaciers and other permafrost deposits represents a substantial reservoir of ground water that has seldom been recognized in alpine terrain. Mean annual air temperatures increased in Loch Vale by 1.1° to 1.4°C during 1992–2000, consistent with longer-term trends at similar high-elevation sites nearby and globally. Increasing air temperatures may raise the lower limit of permafrost, potentially altering the hydrology and vegetation patterns in alpine basins.

The results of this study have implications for evolving conceptual models of hydrology in alpine basins in the western United States and other similar settings. A common early assumption was that alpine catchments in the western United States behave like “Teflon® basins,” and that pollutants released during melting of deep seasonal

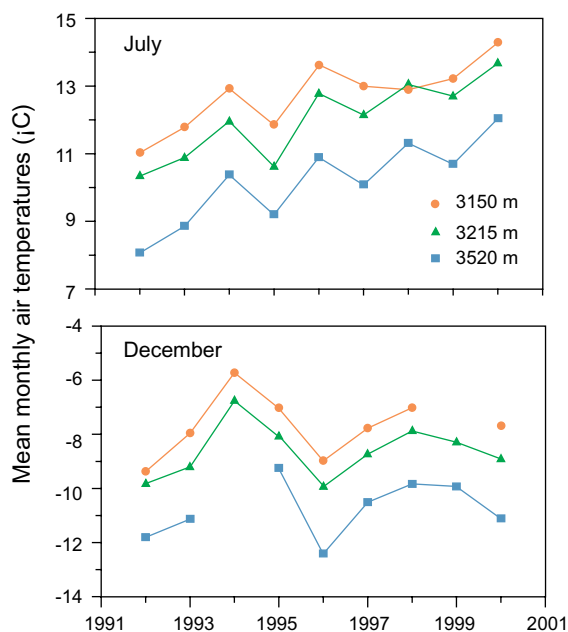


Figure 9. Average monthly air temperature at Loch Vale weather stations. Months with greater than 5% missing values were excluded from the analysis.

snowpacks in the spring (May through June) have little interaction with geologic or biologic materials. This assumption was based on a scarcity of well-developed soils, and because of fast hydrologic flushing rates during snowmelt. It was challenged in the last decade as evidence accumulated that snowmelt and rain were substantially altered by biogeochemical reactions along short flowpaths through talus and/or shallow soil (Williams et al. 1993; Campbell et al. 1995; Mast et al. 1995). The results of this study confirm the role of talus ground water as an important contributor to streamflow, particularly during storm events and during the winter base-flow period.

Acknowledgments

Many thanks to Douglas Hultstrand, Albert Kessler, Dave Manthorne, Irina Overeem, Matthew Reynolds, John Gardner, and Dave Skinner for their assistance in the field. Funding was provided through the U.S. Geological Survey's Water, Energy, and Biogeochemical Budgets program. A grant from the Max Kade Foundation, New York to Lothar Schrott is greatly appreciated.

Authors' Note: The use of firm, trade, and brand names in this article is for identification purposes only and does not constitute endorsement by the U.S. government.

Editor's Note: The use of brand names in peer-reviewed papers is for identification purposes only and does not constitute endorsement by the authors, their employers, or the National Ground Water Association.

References

- Arthur, M. 1992. Vegetation. In *Biogeochemistry of an Alpine Ecosystem*, ed. J. Baron, 76–92. New York: Springer-Verlag.
- Bachmann, S.A. 1994. Hydrology of a subalpine wetland complex in Rocky Mountain National Park, Colorado. M.S. thesis, Department of Earth Resources, Colorado State University, Fort Collins, Colorado.
- Ballantyne, C.K. 1998. Age and significance of mountain-top detritus. *Permafrost and Periglacial Processes* 9, 327–345.
- Baron, J. 1992. *Biogeochemistry of a Subalpine Ecosystem*. New York: Springer-Verlag.
- Baron, J., and A.S. Denning. 1992. Hydrologic budget estimates. In *Biogeochemistry of an Alpine Ecosystem*, ed. J. Baron, 28–47. New York: Springer-Verlag.
- Baron, J., and A.S. Denning. 1993. The influence of mountain meteorology on precipitation chemistry at low and high elevations of the Colorado Front Range, USA. *Atmospheric Environment*, 27A, no. 15: 2337–2349.
- Barsch, D. 1978. Active rock glaciers as indicators for discontinuous permafrost: An example from the Swiss Alps. In *Proceedings of Third International Conference on Permafrost, Ottawa, Canada*, 349–353. Ottawa, Canada: International Permafrost Association.
- Barsch, D. 1988. Rockglaciers. In *Advances in Periglacial Geomorphology*, ed. M.J. Clark, 69–90. New York: John Wiley and Sons.
- Battin, T.J. 1999. Hydrologic flow paths control dissolved organic carbon fluxes and metabolism in an alpine stream hyporheic zone. *Water Resources Research* 35, no. 10: 3159–3169.
- Bencala, K.E., and R.A. Walters. 1983. Simulation of solute transport in a mountain pool-and-riffle stream: A transient storage model. *Water Resources Research* 19, no. 3: 718–724.
- Boulton, A.J., S. Findlay, P. Marmonier, E.H. Stanley, and H.M. Valett. 1998. The functional significance of the hyporheic zone in streams and rivers. *Annual Review of Ecological Systems* 29, 59–81.
- Braddock, W.A., and J.C. Cole. 1990. Geologic map of Rocky Mountain National Park and Vicinity, Colorado. U.S. Geological Survey 1:50,000.
- Broshears, R.E., K.E. Bencala, B.A. Kimball, and D.M. Mcknight. 1993. Tracer-dilution experiments and solute-transport simulation for a mountain stream, Saint Kevin Gulch, Colorado. U.S. Geological Survey Water Resources Investigation Report 92–4081.
- Campbell, D.H., J.S. Baron, K.A. Tonnessen, P.D. Brooks, and P.F. Schuster. 2000. Controls on nitrogen flux in alpine/sub-alpine watersheds of Colorado. *Water Resources Research* 36, no. 1: 37–47.
- Campbell, D.H., D.W. Clow, G.P. Ingersoll, M.A. Mast, N.E. Spahr, and J.T. Turk. 1995. Processes controlling the chemistry of two snowmelt-dominated streams in the Rocky Mountains. *Water Resources Research* 31, no. 11: 2811–2821.
- Davinroy, T. 2000. Hydrologic and biogeochemical characteristics of alpine talus, Colorado Front Range. Ph.D. dissertation, Department of Geography, University of Colorado, Boulder.
- Davis, S.N. 1969. Porosity and permeability in natural materials. In *Flow Through Porous Media*, ed. R.J.M. DeWiest, 53–89. New York: Academic Press.
- Dyurgerov, M.B., and M.F. Meier. 2000. Twentieth century climate change: Evidence from small glaciers. *Proceedings of the National Academies of Science* 97, no. 4: 1406–1411.
- Fetter, C.W. 2001. *Applied Hydrogeology*, 4th ed. Upper Saddle River, New Jersey: Prentice-Hall.
- Frew, J. 1990. The Image Processing Workbench. Ph.D. dissertation, Department of Geography, University of California, Santa Barbara.
- Funk, M., and M. Hoelzle. 1992. A model of potential direct solar radiation for investigating occurrences of mountain permafrost. *Permafrost and Periglacial Processes* 3, 139–142.
- Gable, D.J., and R.F. Madole. 1976. Geologic map of the Ward quadrangle, Boulder County, Colorado. U.S. Geological Survey, 1:24,000.
- Haerberli, W., and M. Beniston. 1998. Climate changes and its impacts on glaciers and permafrost in the Alps. *Ambio* 27, no. 4: 258–265.
- Haerberli, W., C. Gouodong, A.P. Gorbunov, and S.A. Harris. 1993. Mountain permafrost and climatic change. *Permafrost and Periglacial Processes* 4, 165–174.
- Harris, S.A., and A.E. Corte. 1992. Interactions and relations between mountain permafrost, glaciers, snow and water. *Permafrost and Periglacial Processes* 3, 103–110.
- Hirsch, R.M., J.R. Slack, and R.A. Smith. 1982. Techniques of trend analysis for monthly water quality data. *Water Resources Research* 18, no. 1: 107–121.
- Hoelzle, M., and W. Haerberli. 1995. Simulating the effects of mean annual air temperature changes on permafrost distribution and glacier size: An example from the Upper Engadin, Swiss Alps. *Annals of Glaciology* 21, 399–405.
- Intergovernmental Panel on Climate Change. 2001. *Climate Change 2001: The Scientific Basis*. Geneva, Switzerland: IPCC.
- Ives, J. 1973. Permafrost and its relationship to other environmental parameters in a midlatitude, high-altitude setting, Front Range, Colorado Rocky Mountains. In *Proceedings of Permafrost: The North American Contribution to the Second International Conference*, Washington, D.C., 121–125. Washington, D.C.: National Academy of Science.
- Kattlemann, R. 1989. Groundwater contributions in an alpine basin in the Sierra Nevada. In *Proceedings of Symposium on Headwaters Hydrology*, 361–369. Herndon, Virginia: American Water Resources Association.

- Kattlemann, R., and K. Elder. 1991. Hydrologic characteristics and water balance of an alpine basin in the Sierra Nevada. *Water Resources Research* 27, no. 7: 1553–1562.
- Keller, F., and H. Gubler. 1993. Interaction between snow cover and high mountain permafrost, Murtel-Corvatsch, Swiss Alps. In *Proceedings of Sixth International Conference on Permafrost*, 332–337. Beijing: International Permafrost Association.
- Lautridou, J.-P. 1988. Recent advances in cryogenic weathering. In *Advances in Periglacial Geomorphology*, ed. M.J. Clark, 33–47. New York: John Wiley and Sons.
- Masch, F.D., and K.J. Denny. 1966. Grain-size distribution and its effect on the permeability of unconsolidated sands. *Water Resources Research* 2, no. 4: 665–677.
- Mast, M.A., C. Kendall, D.H. Campbell, D.W. Clow, and J. Back. 1995. Determination of hydrologic pathways in an alpine-subalpine basin using isotopic and chemical tracers. In *Biogeochemistry of Seasonally Snow-Covered Catchments*, ed. K. Tonnessen, M. Williams, and M. Tranter, 263–270. Boulder, Colorado: International Association of Hydrological Sciences.
- Pierson, T.C. 1982. Classification and hydrological characteristics of scree slope deposits in the Northern Craigieburn Range, New Zealand. *Journal of Hydrology (N.Z.)* 21, no. 1: 34–59.
- Rantz, S.E. 1982. Measurement and computation of streamflow: Volume 1. Measurement of stage and discharge. U.S. Geological Survey Water-Supply Paper 2175.
- Reynolds, J.M. 1997. *An Introduction to Applied and Environmental Geophysics*. Chichester: Wiley.
- Runkel, R.L. 1998. One-dimensional transport with inflow and storage (OTIS): A solute transport model for stream and rivers. U.S. Geological Survey Water Resources Investigations Report 98–4018.
- Sandmeier, K.-J. 1998. ReflexW. Program for the processing of seismic, acoustic or electromagnetic reflection, refraction and transmission data. Karlsruhe, Germany: Sandmeier Software.
- Schrott, L. 1996. Some geomorphological-hydrological aspects of rock glaciers in the Andes (San Juan, Argentina). *Zoological Geomorphology* 104, 161–173.
- Schrott, L., G. Hufschmidt, M. Hankammer, T. Hoffmann, and R. Dikau. Spatial distribution of sediment storage types and quantification of valley fill deposits in an alpine basin, Reintal, Bavarian Alps, Germany. *Geomorphology* 55, 45–63.
- Snow, D.T. 1968. Hydraulic character of fractured metamorphic rocks of the Front Range and implications to the Rocky Mountain Arsenal Well. *Colorado School of Mines Quarterly* 63, no. 1: 167–199.
- Swift, L.W.J. 1976. Algorithm for solar radiation on mountain slopes. *Water Resources Research* 12, no. 1: 108–112.
- Vitvar, T., D.A. Burns, G.B. Lawrence, J.J. McDonnell, and D.M. Wolock. 2002. Estimation of baseflow residence times in watersheds from the runoff hydrograph recession: Method and application in the Neversink watershed, Catskill Mountains, New York. *Hydrological Processes* 16, 1871–1877.
- Vuille, M., and R.S. Bradley. 2000. Mean annual temperature trends and their vertical structure in the tropical Andes. *Geophysical Research Letters* 27, no. 23: 3885–3888.
- Wang, S.L., H.J. Jin, S. Li, and L. Zhao. 2000. Permafrost degradation on the Qinghai-Tibet Plateau and its environmental impacts. *Permafrost and Periglacial Processes* 11, 43–53.
- Williams, M.W., J. Baron, N. Caine, and R. Sommerfeld. 1996a. Nitrogen saturation in the Rocky Mountains. *Environmental Science & Technology* 30, 640–646.
- Williams, M.W., M. Losleben, N. Caine, and D. Greenland. 1996b. Changes in climate and hydrochemical responses in a high-elevation catchment in the Rocky Mountains, USA. *Limnology & Oceanography* 41, no. 5: 939–946.
- Williams, M.W., A.D. Brown, and J.M. Melack. 1993. Geochemical and hydrologic controls on the composition of surface water in a high-elevation basin, Sierra Nevada, California. *Limnology & Oceanography* 38, no. 4: 775–797.